Immunology Letters 255 (2023) 21–31

Contents lists available at ScienceDirect

Immunology Letters

journal homepage: www.elsevier.com/locate/immlet

Musculin does not modulate the disease course of Experimental Autoimmune Encephalomyelitis and DSS colitis

Anna Vanni [a], Alberto Carnasciali [a], Alessio Mazzoni [a], Edda Russo [a], Parham Farahvachi [a], Leandro Di Gloria [b], Matteo Ramazzotti [b], Giulia Lamacchia [a], Manuela Capone [a], Lorenzo Salvati [a], Laura Calosi [a], Daniele Bani [a], Francesco Liotta [a], Lorenzo Cosmi [a], Amedeo Amedei [a], Clara Ballerini [a], Laura Maggi [a,*], Francesco Annunziato [a]

[a] Department of Experimental and Clinical Medicine, University of Florence, Florence 50139, Italy
[b] Department of Biomedical, Experimental and Clinical Sciences "Mario Serio", University of Florence, Florence 50139, Italy

ARTICLE INFO

Keywords:
Multiple sclerosis
EAE
Inflammation
Th17
Musculin
IL-2
DSS
Colitis
Microbiota

ABSTRACT

Previous evidences show that *Musculin* (*Msc*), a repressor member of basic helix-loop-helix transcription factors, is responsible *in vitro* for the low responsiveness of human Th17 cells to the growth factor IL-2, providing an explanation for Th17 cells rarity in inflammatory tissue. However, how and to what extent *Musculin* gene can regulate the immune response *in vivo* in an inflammatory context is still unknown. Here, exploiting two animal models of inflammatory diseases, the Experimental Autoimmune Encephalomyelitis (EAE) and the dextran sodium sulfate (DSS)-induced colitis, we evaluated the effect of *Musculin* gene knock-out on clinical course, performing also a deep immune phenotypical analysis on T cells compartment and an extended microbiota analysis in colitis-sick mice. We found that, at least during the early phase, *Musculin* gene has a very marginal role in modulating both the diseases. Indeed, the clinical course and the histological analysis showed no differences between wild type and *Msc* knock-out mice, whereas immune system appeared to give rise to a regulatory milieu in lymph nodes of EAE mice and in the spleen of DSS colitis-sick mice. Moreover, in the microbiota analysis, we found irrelevant differences between wild type and *Musculin* knock-out colitis-sick mice, with a similar bacterial strains' frequency and diversity after the DSS treatment. This work strengthened the idea of a negligible *Msc* gene involvement in these models.

1. Introduction

Chronic inflammatory disorders are a heterogeneous group of diseases characterized by uncontrolled, persistent inflammation at target organs, leading to impaired functionality and disability. Deregulated innate and adaptive immune responses are responsible for sustained inflammation, and targeting inflammatory cells, or their products, is an effective strategy in alleviating disease symptoms [1]. For this reason, understanding the basic biology of immune cells activation and regulation is of relevant importance to define which pathways are altered in chronic inflammation, thus potentially providing novel targets for therapy.

Transcription factors belonging to the basic helix-loop-helix (bHLH) family are a considerable number of proteins involved in a wide array of developmental processes and are master regulators of lymphoid cells' development and differentiation [2]. They commonly work as homo- or hetero-dimers and can activate/ suppress gene expression. E proteins HEB and E2A, which belong to the bHLH family, promote thymocyte development at the double positive stage [3], while their activity must be down-regulated to proceed to the single positive stage [4–6]. Among bHLH members with suppressive activity, Id2 and Id3 are the most studied. These transcription factors play primary roles in $CD4^+$and $CD8^+$

Abbreviations: bHLH, basic helix-loop-helix; CNS, Central Nervous System; CD, cluster of differentiation; DSS, Dextran Sodium Sulphate; EAE, Experimental Autoimmune Encephalomyelitis; FoxP3, Forkhead box P3; H&E, Hematoxylin and Eosin; IL-2, Interleukin-2; IL-10, Interleukin-10; IL-17, Interleukin-17; IL-22, Interleukin-22; IFN-γ, Interferon gamma; LFB/PAS, Luxol Fast Blue/Periodic Acid Schiff's staining; LN, Lymph Node; MOG, Myelin-oligodendrocyte glycoprotein; *Msc*, *Musculin*; PMA, Phorbol Myristate Acetate.

* Corresponding author.
E-mail address: laura.maggi@unifi.it (L. Maggi).

https://doi.org/10.1016/j.imlet.2023.02.006
Received 6 December 2022; Received in revised form 13 February 2023; Accepted 23 February 2023
Available online 26 February 2023

T cell development [7,8]. Another bHLH transcription factor with suppressing activity is *Musculin* (*Msc*, also known as MyoR or ABF-1), which showed the capability to block skeletal myogenesis by repressing MyoD transcription factor [9], to play a protective role for kidney cells in a renal failure murine model [10] and to establish normal cardiac conduction in a Gata4-dependent transcriptional circuit [11]. Furthermore, a prominent *Msc* role in immune system modulation has been suggested after its expression has been described in B cell lymphoma, where it is involved in decreasing the B lymphocyte proliferation and survival [12]. Likewise, *Msc* controls also T cell proliferation since the loss of function mutations of this gene has been observed in anaplastic large cells lymphoma (ALCLs), a common group of T cells non-Hodgkin lymphomas. In this setting, the impaired *Msc* functionality in T cells leads to unrestrained Myc activity, thus promoting cell cycle progression [13]. A similar role has been demonstrated also in Th17 cells, since *Msc* can suppress their IL-2 mediated proliferation by activating a complex mechanism of serine phosphorylation that ultimately impairs STAT5b activity [14]. Importantly, this finding might contribute to explain why Th17 cells have been found to be rare in the inflamed sites of several animal models [15–17] or in human inflammatory and autoimmune diseases, such as Crohn's disease and multiple sclerosis [18–20]. In addition, *Msc* has been recently identified also as a critical factor for induced-Treg (iTreg) development in mice, by suppressing the Th2 differentiation program [21]. With these premises, *Msc* seems to play a primary role in lymphoid cell differentiation and function. However, how *Msc* regulates the immune responses of different cell subsets in the pathogenic, inflammatory, context remains to be completely understood. For this reason, in this work we studied the effect of *Msc* deletion in the development of two well-established murine models of human chronic inflammatory disorders, the Experimental Autoimmune Encephalomyelitis (EAE) and dextran sodium sulfate (DSS)-induced colitis, analyzing for this last model also the intestinal microbiota composition, as a counterpart of the inflammatory process (the gut microbiome-immunity axis) [22]. Our findings demonstrate that *Msc* itself has a negligible impact on the disease course.

2. Materials and methods

2.1. Experimental animals

We used non-littermate C57BL/6-B129 wild type (WT, total n=17) and *Msc*$^{-/-}$ (KO, total n=18) mice, co-housed in the same breeding facility (Charles River, ITALY). During each experimental session, animals were co-housed at the CeSaL animal house of the University of Florence, in Makrolon cages according to the genetic background, with free access to food and water and kept at 23 °C with a 12 h light/dark cycle. Every manipulation of the animals was executed according to the guidelines of the European community for animal care (DL 116/92, application of the European Communities Council Directive 2010/63/EU) and approved by the Committee for Animal Care (DGSAF, Italy, Authorization no. 798/2018-PR)".

2.2. EAE induction

EAE was induced in 8 to 10 weeks-old female mice (WT, n= 17) and *Msc* $^{-/-}$ (KO, n=18) by subcutaneous (s.c.) injection of 200 μg of myelin oligodendrocyte glycoprotein $MOG_{35–55}$ peptide (MEVGWYRSPFSRVVHLYRNGK, purity 85%; Espikem, Florence, Italy) in Phosphate Buffer Saline solution (PBS, Carlo Erba Reagents S.r.l., Italy), emulsified with an equal volume of complete Freund's adjuvant (CFA, Sigma) supplemented with 7 mg/mL^{-1} *Mycobacterium tuberculosis* H37Ra (Difco Laboratories, USA). *Bordetella pertussis* toxin (500 ng) was administered by i.p. injection at days 0 and 2 post immunization (Merck, Germany). All the experiments with animals were performed blinded and mice were randomly assigned to the experimental groups. EAE-induced mice were scored daily for clinical signs of disease, according to the following scale: (0) normal mouse, no overt signs of disease; (1) limp tail or hind limb weakness but not both; (2) limp tail and hind limb weakness; (3) partial hind limb paralysis; (4) complete hind limb paralysis; (5) moribund state or death by EAE: sacrifice for humane reasons.

2.3. DSS colitis induction

Colitis was induced in 8 to 10 weeks-old male mice (WT, n= 6) and *MSC* $^{-/-}$ (KO, n=6) by feeding them with 3% DSS 40,000 kDa (Sigma, Germany) in water for 8 days. Mice were daily weighted until the day of sacrifice.

2.4. Feces collection and 16S rRNA V3-V4 region gene sequencing and sequencing data analysis

Fresh feces from four WT and four KO mice were collected at T0 (pre-DSS treatment) and T1 (post-DSS treatment) and were stored at −80 °C until analysis. Fecal bacterial DNA extraction was performed as described in our previous study [23]. The 16S rRNA gene V3-V4 region was amplified from genomic DNA using the universal bacterial primers 341F and 805R. The amplicons were normalized, pooled and sequenced on the Illumina MiSeq sequencer. Libraries were prepared using Library Quant Kit Illumina GA revised primer-SYBR Fast Universal (KAPA, Wilmington, MA, USA) and sequenced for 600 cycles on an Illumina MiSeq using the MiSeq Reagent Kit (Illumina, San Diego, CA, USA) at IGA technology service (Udine). Primer trimming, denoising, high-quality sequence merging and ASV delineation were performed using Cutadapt and DADA2 in the QIIME2 v2021.4 environment. The scikit-learn classifier retrained on the V3-V4 region of the SILVA138 database has been used for the taxonomic assignment [24]. Further details regarding sequence processing and analysis is available on GitHub (see https://github.com/LeandroD94/Papers). Microbiota raw and processed data has been publicly deposited in NCBI GEO database under accession GSE223002.

2.5. Histology

Immediately after the sacrifice, the spinal cord from EAE mice and the colon from colitis-sick mice were carefully removed and put in PBS for 3 h. Later, tissue samples were fixed with 4% paraformaldehyde (PFA) and paraffin-embedded and sectioned with a microtome in 5 μm thick slices. Alternatively, tissue sections were embedded in Optimal Cutting Temperature compound (OCT) (Bio-Optica, Italy), frozen at -80 °C, and cut with a microtome-cryostat. Afterwards, slices were stained with Hematoxylin and Eosin (H&E) or Luxol Fast Blue/Periodic Acid-Schiff (LFB/PAS), following standard protocols. The number of inflammatory infiltrates and demyelinated areas in the spinal cord were evaluated by a manual count on a selected or fixed area in EAE mice, using a 4X magnification with microscope (Leica DM750, Germany). With the same approach, inflammatory infiltrates into the colonic mucosa and submucosal areas were evaluated in colitis-sick mice.

2.6. Tissue processing

After the sacrifice, spleen, inguinal and axillary lymph nodes and spinal cord were carefully removed and promptly put in PBS with Penicillin/Streptomycin 1%. Afterwards, all tissues were smashed on a nylon 22 μm filter (Corning, USA) and different protocols were used for each organ: mononucleated cells were isolated after density gradient centrifugation (Lymphoprep, Stem Cell, USA) from collected splenocytes; cells from lymph nodes directly underwent to flow cytometry staining; spinal cord mononucleated cells were isolated by means of Percoll (GE Healthcare, USA) density gradient centrifugation.

2.7. Flow cytometry

Staining for intranuclear FoxP3^{+}and Ki-67 was performed on each organ following manufacturer's protocol (e-Bioscience, USA) using fluorochrome-conjugated antibodies listed in Table 1. Intracellular staining was performed by restimulating cells *ex vivo* with PMA and Ionomycin. After two hours of incubation at 37 °C, 5% CO_2, cells were treated with Brefeldin-A (5 μg/mL), followed by additional 3 h of incubation. Finally, cells were fixed and stained using fluorochrome-conjugated antibodies listed in Table 2. Samples were acquired on a BD LSR II flow cytometer (BD Biosciences) with FACS Diva Software and analyzed by FlowJo Software. Membrane staining was performed using the antibodies listed in Table 3.

2.8. Absolute cell number

Absolute cells number from the spleen and colon of WT and KO mice were counted using a MACS Quant (Miltenyi Biotech, Germany).

3. Results

3.1. Msc knock-out did not impact the EAE clinical outcome and histological features

To understand if *Msc* deletion affects EAE outcome, we firstly evaluated the clinical progression of *Msc*$^{-/-}$ (n=18) compared to WT B6/129 (n=17) EAE mice, attributing a clinical score which ranges from 1 to 5, as described in the methods section. The clinical score showed no differences between the groups (Fig. 1A) and the disease developed equally in both conditions, with initial disability occurring around day 8 post-immunization (Fig. 1A). The kinetics of disease development was similar for *Msc*$^{-/-}$ and WT mice, with a maximum score on day 15, requiring to euthanize mice for the high score reached. Furthermore, clinical observations were corroborated by histological analysis performed on spinal cord sections, where hematoxylin and eosin staining showed that the extent of inflammatory infiltrates was comparable between *Msc*$^{-/-}$ mice and WT (Fig. 1 B–E and J), as well as demyelinated areas evaluated by Luxol Fast Blue staining (Fig. 1 F–I and K).

3.2. WT and Msc$^{-/-}$ mice showed comparable numbers of CNS immune infiltrates

As EAE is an autoimmune disease characterized by focal infiltration of immune cells in the CNS [25], we performed an extended flow cytometry phenotypical analysis, in order to define the composition of the immune subpopulations throughout the CNS, using the spleen and lymph nodes as reference organs. Flow cytometric analysis allowed the identification of monocytes, divided into classical CD64^{+}Lc6y^{high} and non-classical CD64^{+}Lc6y^{dim} monocytes, eosinophils, neutrophils, and B and T cells. Focusing on cells infiltrating the CNS, we observed no difference in the total absolute number of B, T, CD4^{+} T and CD8^{+} T cells in *Msc*$^{-/-}$ compared to WT mice (Fig. 2B). The same result was obtained by evaluating myeloid infiltrate, as the absolute number of monocytes, eosinophils and neutrophils appeared comparable between WT and *Msc*$^{-/-}$ mice as well (Fig. 2A). Likewise, comparable cellularity in the two experimental groups was found in the spleen (Fig. 2C and D) and also in the lymph nodes (Fig. 2E and F).

Table 1
List of fluorochrome-conjugated antibodies used for intracellular staining of FoxP3 and Ki-67.

Antigen	Fluorochrome	Clone	Company
Ki-67	FITC	SolA15	eBioscience™
CD4	PE	RM4–5	eBioscience™
CD3	SB600	145–2C11	eBioscience™
CD8	BV711	53–6.7	BDBioscience
FoxP3	eFluor450	FJK-16s	eBioscience™
L/D	Fixable Viability Stain 780		BDBioscience
CD25	APC	7D4	Miltenyi Biotec

Table 2
List of fluorochrome-conjugated antibodies used for flow cytometric evaluation of T cells cytokine production.

Antigen	Fluorochrome	Clone	Company
IL17	Alexa Fluor 488	TC11–18H10	BDBioscience
IL10	PE	JES516E3	eBioscience™
IFNγ	PerCP-Cy5.5	XMG1.2	eBioscience™
CD3	SB600	145–2C11	eBioscience™
CD8	BV711	53–6.7	BDBioscience
L/D	Fixable Viability Stain 780		BDBioscience
CD4	PE-Cy7	RM4–5	eBioscience™
IL22	APC	IL22JOP	eBioscience™

Table 3
List of all fluorochrome-conjugated antibodies used for flow cytometric immunophenotyping of lymphoid and mieloid cells.

Antigen	Fluorochrome	Clone	Company
CD19	FITC	6D5	Miltenyi Biotec
CD8	PE	53–6.7	Miltenyi Biotec
Siglec-F	PE	E50–2440	BDBioscience
LY6G	PerCP-Cy5.5	1A8	BioLegend
Ly6C	Pacific Blue	HK1.4	BioLegend
CD3	APC-eFluor780	145–2C11	eBioscience™
CD4	PE-Cy7	RM4–5	eBioscience™
CD64	APC	X54.5/7.1	eBioscience™

3.3. Functional characterization of T cells showed a rising regulatory milieu in the peripheral lymph nodes of Msc$^{-/-}$ mice

We also evaluated by flow cytometry the frequency of Treg lymphocytes, defined as Foxp3^{+}CD25^{+}, in *Msc*$^{-/-}$ and WT mice. Of note, *Msc*$^{-/-}$ mice showed a significant higher frequency of Treg in lymph nodes than WT mice (Fig. 2G). Conversely, the spleen and CNS showed a comparable percentage of regulatory T cells between the two experimental groups (Fig. 2G).

Data obtained so far showed no major differences in immune cells infiltrating the spinal cord in *Msc*$^{-/-}$ mice compared to WT. In order to characterize the functional properties of T cells in our experimental group, we monitored the expression of Ki-67, a proliferation marker, and cytokines production. No differences were observed between *Msc* $^{-/-}$ and WT mice for Ki-67 expression by CD4^{+} and CD8^{+} T cells throughout the tissue considered, suggesting a similar proliferation rate in both the groups (Fig. 3A and B). However, it should be noted that Ki-67 identifies all cells in G1-S-M phases, but provides no information regarding the speed of cycling.

Further, we investigated the capability to produce IL-17, IFN-γ, IL-10 and IL-22 cytokines in CD4^{+} and CD8^{+}T lymphocytes infiltrating the CNS.

The IFN-γ, IL-17, IL-22 and IL-10 production by CD4^{+}T cells showed no statistically significant differences between *Msc*$^{-/-}$ and WT mice in CNS (Fig. 3C). Nevertheless, analyzing the CD4^{+} cytokines secretion in the reference organs, we found a significantly reduced production of IL-17 in cells derived from lymph nodes of *Msc*$^{-/-}$ mice (Fig. 3G). No differences were observed in the levels of the remaining analyzed cytokines and in the spleen (Fig. 3E).

The same analysis was also performed on CD8^{+} T cells. We observed comparable levels of all analyzed cytokines in CNS-derived cells from both WT and *Msc*$^{-/-}$ mice (Fig. 3D). Notably, *Msc*$^{-/-}$ CD8^{+} T cells from lymph nodes produced lower IL-10 and IFN-γ than WT mice (Fig. 3H), while no difference in cytokines production was observed in CD8^{+} T cells derived from the spleen in both experimental groups (Fig. 3F).

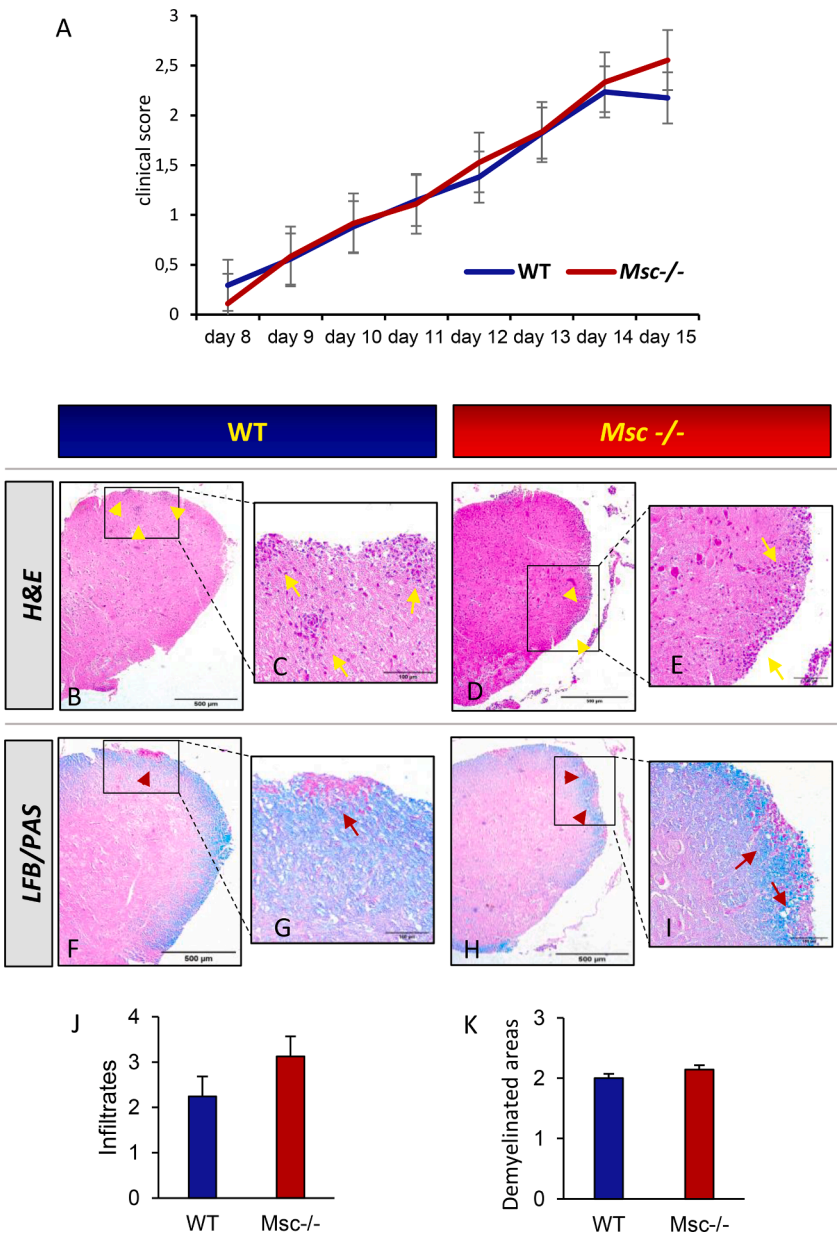

Fig. 1. *Similar EAE clinical score and spinal cord pathology in $Msc^{-/-}$ mice and wild type (WT) mice.* (A) EAE clinical score evaluated daily in $Msc^{-/-}$ (n=18, red line) and WT (n=17, blue line) according to following scale: 0 normal mouse, no overt signs of disease; 1 limp tail or hind limb weakness but not both; 2 limp tail and hind limb weakness; 3 partial hind limb paralysis; 4 complete hind limb paralysis; 5 moribund state, death by EAE. Mice were scored from day 8 after immunization and sacrificed at day 15 for ethical reasons due to the high score reached. Means ± SE values are reported; Mann–Whitney test was used. (B-I) EAE spinal cord pathology. Panels show representative images, for each group, of spinal cord section after hematoxylin and eosin staining for inflammatory infiltrates in WT and $Msc^{-/-}$ mice (yellow arrows; B, D: 4X scale bar=500 μm; C, E 20X scale bar=100 μm), LFB/ PAS for demyelinated areas in WT and $Msc^{-/-}$ mice (red arrows; F, H: 4X scale bar=500 μm; G, I: 20X, scale bar=100 μm); means ± SD are shown. (J) Number of inflammatory infiltrates in the spinal cord: 7 tissue/sections per mouse were analyzed for each experimental group, in three independent experiments; means ± SD are reported. (K) Number of demyelinated areas in the spinal cord. 5 tissue/sections per mouse were analyzed for each experimental group, in three independent experiments. Means ± SD are reported; Mann–Whitney test was used.

3.4. Musculin did not affect DSS colitis clinical outcome and cytokines production in the colon

Further, we investigated, with the same approach, the involvement of *Msc* gene in another condition of chronic inflammation, the DSS-induced colitis model for human intestinal bowel disease. After inducing colitis in WT (n= 6) and $Msc^{-/-}$ (n= 6) B6/129 mice with dextran sulfate sodium, we followed the weight changes every day, observing a gradual weight reduction from day 5 after treatment beginning, evolving with similar kinetics in both groups, with a maximum reached on day 8. The evaluation of body weight loss showed no differences between the analyzed groups (Fig. 4A).

Given that a characteristic of intestinal inflammation is the thickening and shortening of the large bowel, we measured in mice the colon weight/length ratio. In accordance with the similar weight loss, $Msc^{-/-}$ mice showed equivalent values of colon weight/length ratio to WT (Fig. 4B). Clinical observations were partially confirmed by histological analysis in the colon mucosa. Indeed, hematoxylin and eosin staining (Fig. 4C) and the assigned histological score showed a similar mucosal infiltration between the two groups. On the other hand, submucosal infiltration was significantly lower in $Msc^{-/-}$ mice (Fig. 4D).

Adopting the same approach used in the EAE model, we investigated the immunological characteristic of DSS treated $Msc^{-/-}$ and WT mice. In accordance with a comparable disease course, we observed no differences regarding the immune cell infiltrates in the colon and in the spleen, with similar absolute numbers of myeloid and lymphoid cells, comprising also regulatory T cells, in both the experimental groups (Fig. 5A–D). Moreover, as observed in EAE mice, no differences emerged in $FoxP3^{+}CD25^{+}$ cells frequency neither in the spleen nor in the colon (Fig. 5E).

We further evaluated the colon infiltrating T cells' functionality through the Ki-67 expression and the production of cytokines by flow cytometry. No difference was observed in the frequency of both $CD4^{+}$and $CD8^{+}$ T cells expressing Ki-67, suggesting a similar proliferation rate in the two groups (Fig. 6A and B). Likewise, the levels of cytokines produced by $CD4^{+}$ and $CD8^{+}$ colon infiltrating T cells were comparable in $Msc^{-/-}$ and WT mice (Fig. 6C and D). $CD8^{+}$ T cells obtained from the $Msc^{-/-}$ spleen produced lower levels of IL-10 and IFN-γ

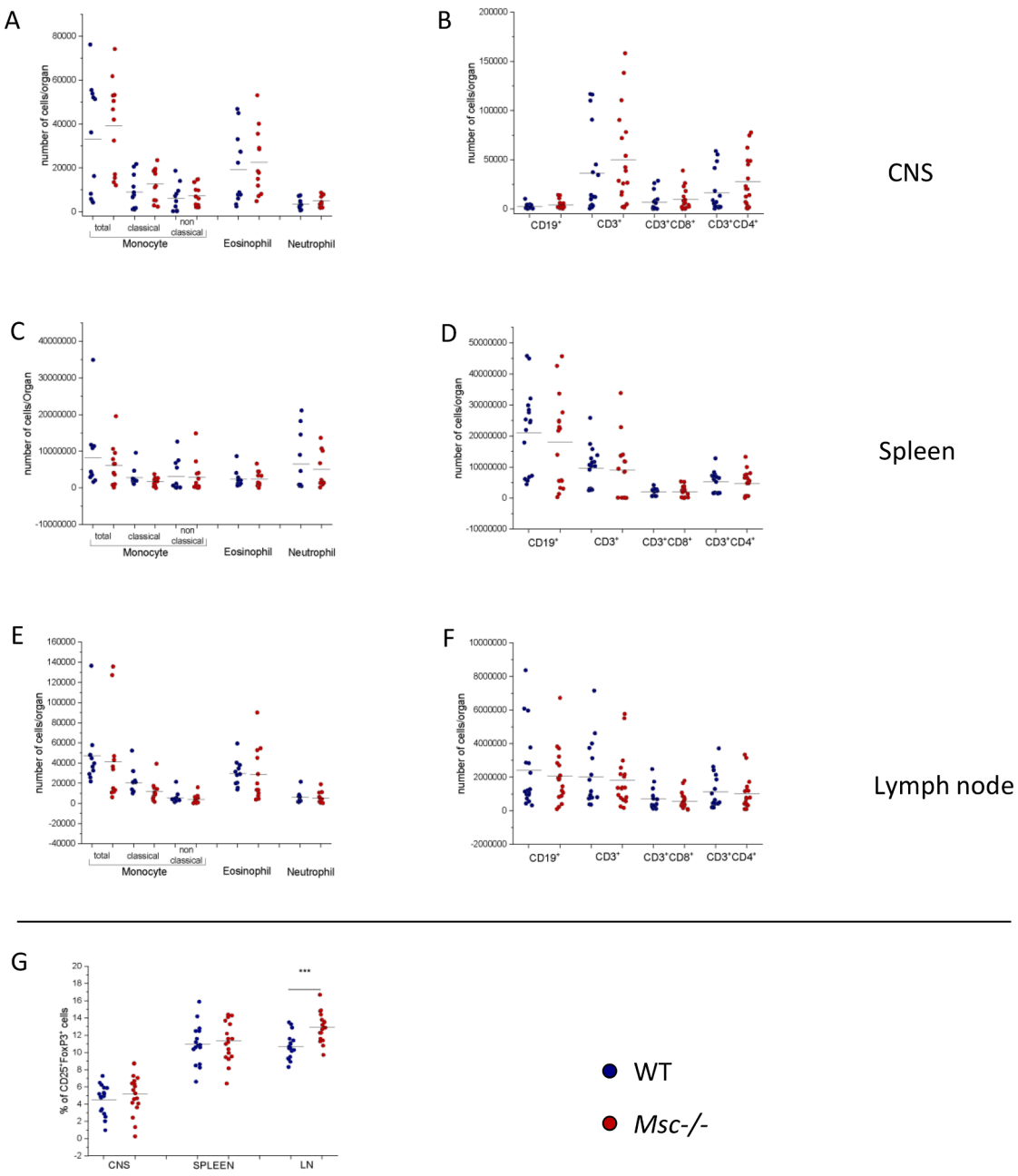

Fig. 2. *Msc gene knock-out does not impact the absolute cell number in CNS, spleen and lymph nodes in EAE compared to WT EAE mice.* Panel shows the absolute cell number belonging to myeloid lineage (A, top, CNS; C, mid, spleen; E, bottom, lymph node) in *Msc*$^{-/-}$ (n=12, red dots) and WT (n=11, blue dots) or to lymphoid lineage (B, top, CNS; D, mid, spleen; F, bottom, lymph node) in *Msc*$^{-/-}$ (n=18, red dots) and WT (n=17, blue dots) evaluated by means of a volumetric count at MACSquant® analyzer. (G) Percentage of FoxP3^{+}CD25^{+} cells in CNS (left), spleen (mid), lymph node (right) in *Msc*$^{-/-}$ (n=18, red dots) and WT (n=17, blue dots). Horizontal black lines represent the mean value; Mann–Whitney test was used (***p < 0.001).

cytokines than WT (Fig. 6F). On the other hand, CD4^{+}T cells showed no differences in the production level of the analyzed cytokines (Fig. 6E).

3.5. *Msc* knock-out did not shape the gut microbiota composition, regardless genetic background

As DSS destroys the epithelial barrier and leads to diffuse gut inflammation [13], we performed a restricted microbiota study in the same WT (n=4) and *Msc*$^{-/-}$ (n=4) B6/129 mice, aiming to evaluate potential alterations, attributable to *Musculin* gene, in the modulation of the gut microbiome-immunity axis, before (T0) and after (T1) DSS treatment.

In order to consider the bacterial diversity among groups (in detail, Group 1: WT-T0; Group 2: KO-T0; Group 3: WT-T1; Group 4: KO-T1), we evaluated the richness and the abundance of microbiota. The alpha diversity parameters, determined by means of Observed, Shannon and Evenness indices, were assessed at both T0 and T1. A trend was observed only for Shannon (p=0.057) and Evenness (p=0.057) indices between WT vs *Msc*$^{-/-}$ mice at T0, with a lower, not significant, alpha diversity for the *Msc*$^{-/-}$ group (Fig. 7A). Indices were not significantly different between WT and *Msc*$^{-/-}$ mice at T1 (Fig. 7B). Then, we determined the effect of DSS-induced colitis on microbiota architecture. Comparing T0 vs T1 fecal samples of WT mice, we observed significant differences at the phylum level. Notably, T1 samples were enriched in *Proteobacteria, Gammaproteobacteria* and *Enterobacteriaceae* (Phylum, Class and family, respectively) (Fig. 8A). Likewise, we observed significant differences at

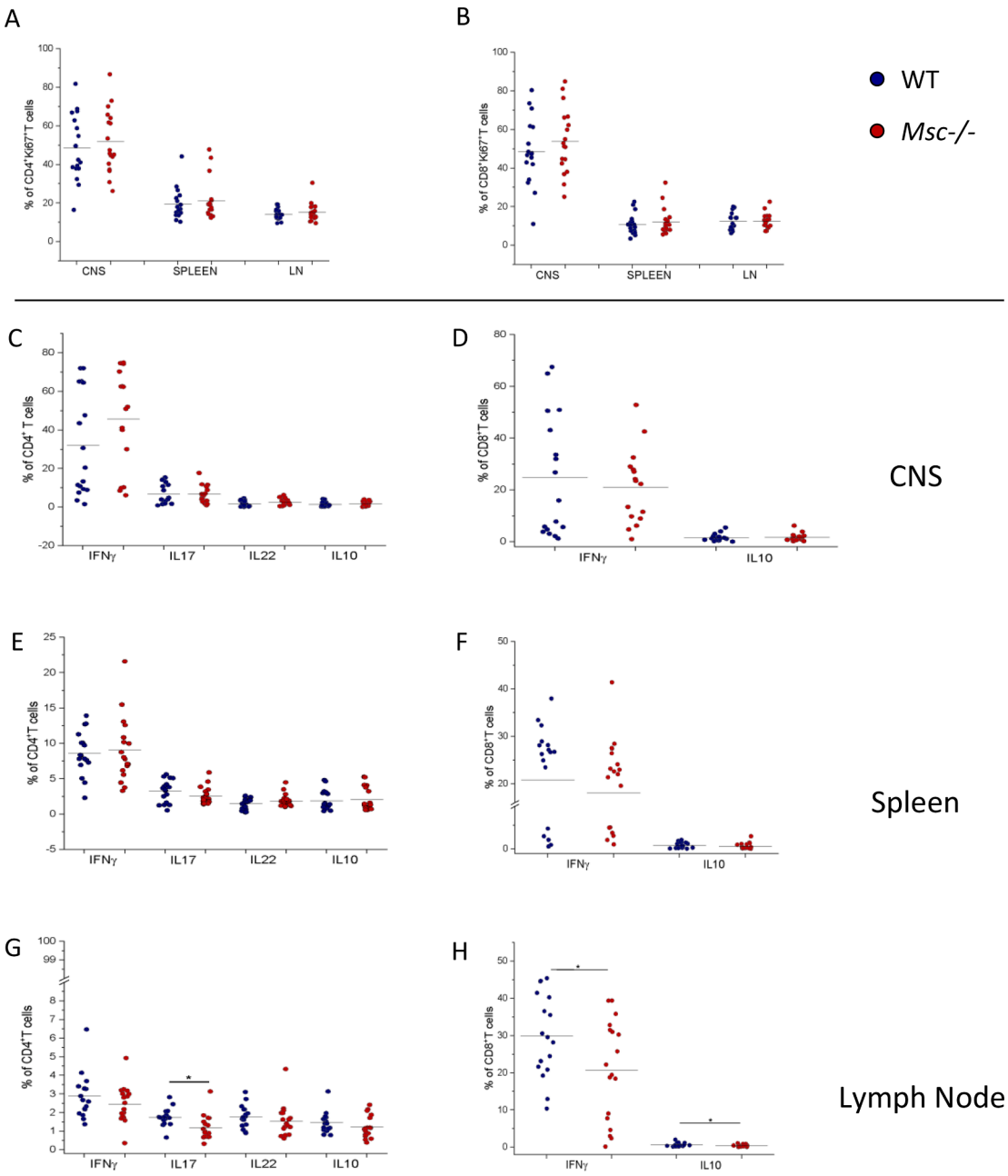

Fig. 3. *Msc gene knock-out does not affect the proliferative capability and cytokines production in CD4+ and CD8+ in CNS, spleen and lymph nodes in EAE compared to WT EAE mice.* Proliferative capability of T cells expressed as percentage of $CD4^{+}Ki\text{-}67^{+}$ T cells (A) and $CD8^{+}Ki\text{-}67^{+}$ T cells (B) from CNS, spleen and lymph node in WT (n=17, blue dots) and $Msc^{-/-}$ (n=18, red dots) EAE mice. (C, E, G) Percentage of total $CD4^{+}$ T or $CD8^{+}$ (D, F, H) T cells producing IL-2, IFN-γ, IL-17 or IL-22 after activation with PMA plus ionomycin and with brefeldin-A in CNS (top), spleen (mid), lymph node (bottom), evaluated by means of intra-cytoplasmatic staining at flow cytometer. Horizontal black lines represent the mean value; Mann–Whitney test was used (*$p < 0.05$).

phylum level in $Msc^{-/-}$ mice. Indeed, T1 samples were enriched in *Proteobacteria, Cyanobacteria* and *Deferribacterota,* while a decrease in *Actinobacterota* was documented (Fig. 8B).

4. Discussion

The purpose of the study was to investigate the effect of *Musculin* gene deletion in two distinct models of inflammation, establishing a possible causal relationship between *Msc* deletion and the unleashing of pathogenic immune cells, with a worsening of disease course. Indeed, as antigen-activated T cells are able to cross the BBB and contribute to CNS damage upon the EAE induction, we expected a worsened clinical outcome in $Msc^{-/-}$ mice, as a loss of the gene would have allowed an uncontrolled proliferation of pathogenic antigen-activated autoreactive lymphocytes, without the capability to halt such a wave. However, from a clinical and histological point of view, we failed to demonstrate differences in the clinical outcome, as $Msc^{-/-}$ mice did not show a different disease course compared to the WT counterpart, nor a different inflammatory infiltrate burden throughout the spinal cord, meaning that *Msc* knock-out was not sufficient to cease either the recruitment toward the CNS of immune cells and the demyelination.

This aspect was further corroborated by the extensive phenotypical analysis of the immune cells in the CNS, spleen and lymph nodes, which showed a comparable qualitative and quantitative distribution of myeloid and lymphoid lineages in all the compartments.

However, *Msc* has been identified as essential for the development of

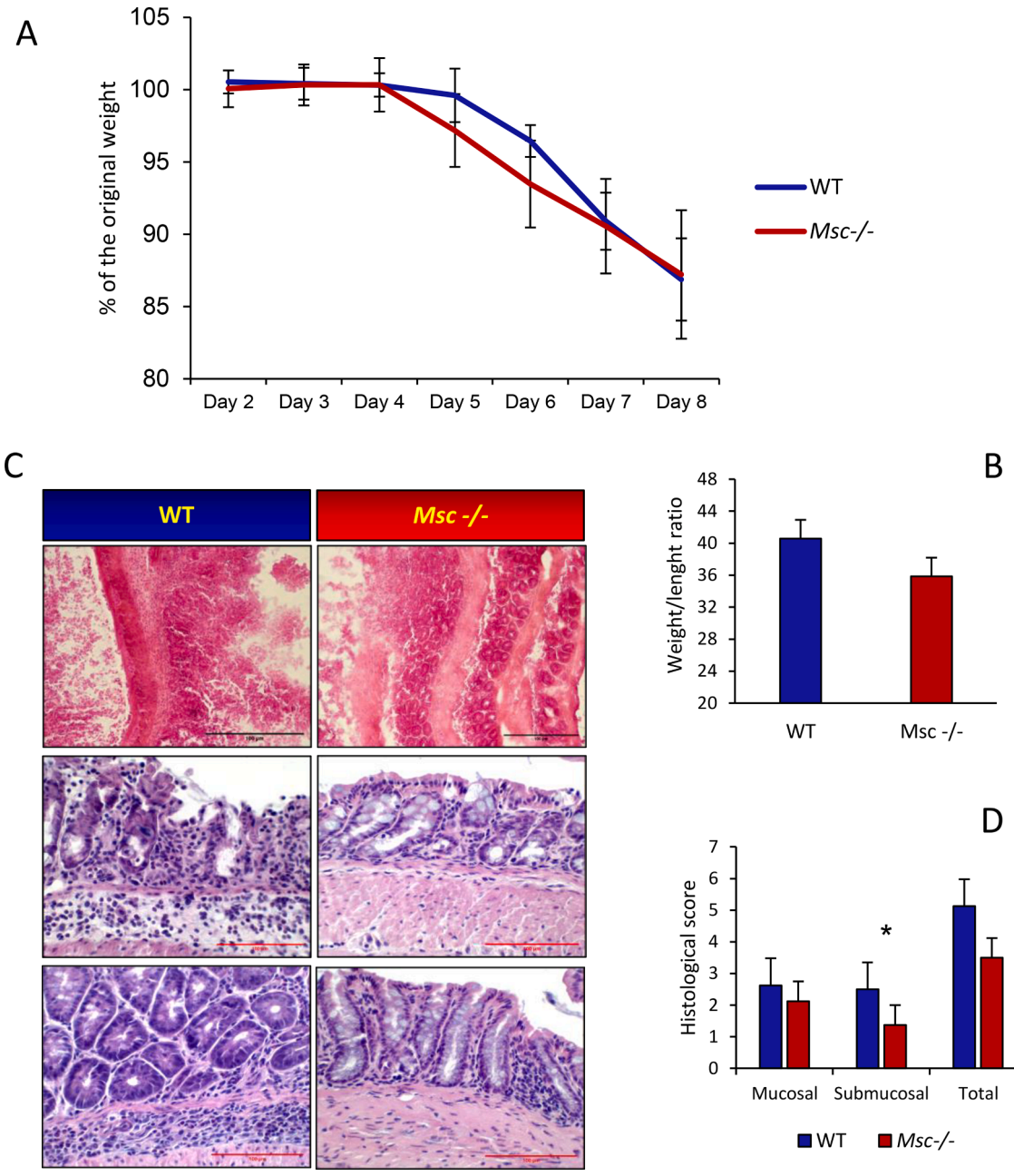

Fig. 4. *Msc gene knock-out does not influence the DSS-induced colitis course but slightly affect the mucosal pathology.* (A) DSS-induced colitis disease course in WT (n=6, blue line) and *Msc*$^{-/-}$ (n=6, red line) from day 2 until the day of sacrifice. Percentage of the original weight (100%) have been reported each day. Values are reported as mean ± SD. (B) Weight/length ratio of colon from WT (n=6, blue column) and *Msc*$^{-/-}$ (n=6, red column) colitis-sick mice. Means ± SD are reported; Mann–Whitney test was used. (C) Panel shows representative images of colon mucosa stained with hematoxylin and eosin (top, cryostat-cut slices, 20X magnification; scale bar=100 μm), (mid and bottom, paraffin-embedded slices, 20X magnification; scale bar=100 μm) in WT (n=5, left side) and *Msc*$^{-/-}$ (n=5, right side) colitis-sick mice. (D) Histological score evaluated by number of inflammatory infiltrates in a fixed area (7 tissue slices per animal) in WT (n=5, blue column) and *Msc*$^{-/-}$ (n=5, red column). Means ± SD are reported; Mann–Whitney test was used (*p < 0.05).

regulatory T lymphocytes from naïve T cells in the periphery and *Msc*$^{-/-}$ mice have been shown to be unable to suppress autoreactive T cells response, causing the spontaneous onset of intestinal and lung inflammation with age [21]. Indeed, it has been demonstrated that the Tregs mediate recovery from EAE by controlling the proliferation of effector myelin-reactive T cells and their traffic towards the CNS [26,27]. However, as we sacrificed the animals after 15 days of disease, we could not further force a speculation about a putative effect of the marginal differences seen in the Treg compartment and cytokines production within peripheral organs, limiting the discussion to a general description.

In the second experimental section, we evaluated the effect of *Msc* gene deletion also in the inflammatory model of DSS-induced colitis, either evaluating the immune system and the microbiota composition of the two experimental groups. In agreement with data obtained in EAE, we did not appreciate differences between colitis-sick WT and *Msc*$^{-/-}$ mice in the disease course. Indeed, the experimental groups showed a similar disease onset, with no alterations in colon weight/length ratio and no differences in function and composition of colon-infiltrating immune cells. Our findings are in contrast with previous studies conducted on DSS colitis mice, where *Msc* knock-out has been repeatedly associated with a worse disease course, a more severe colonic epithelial

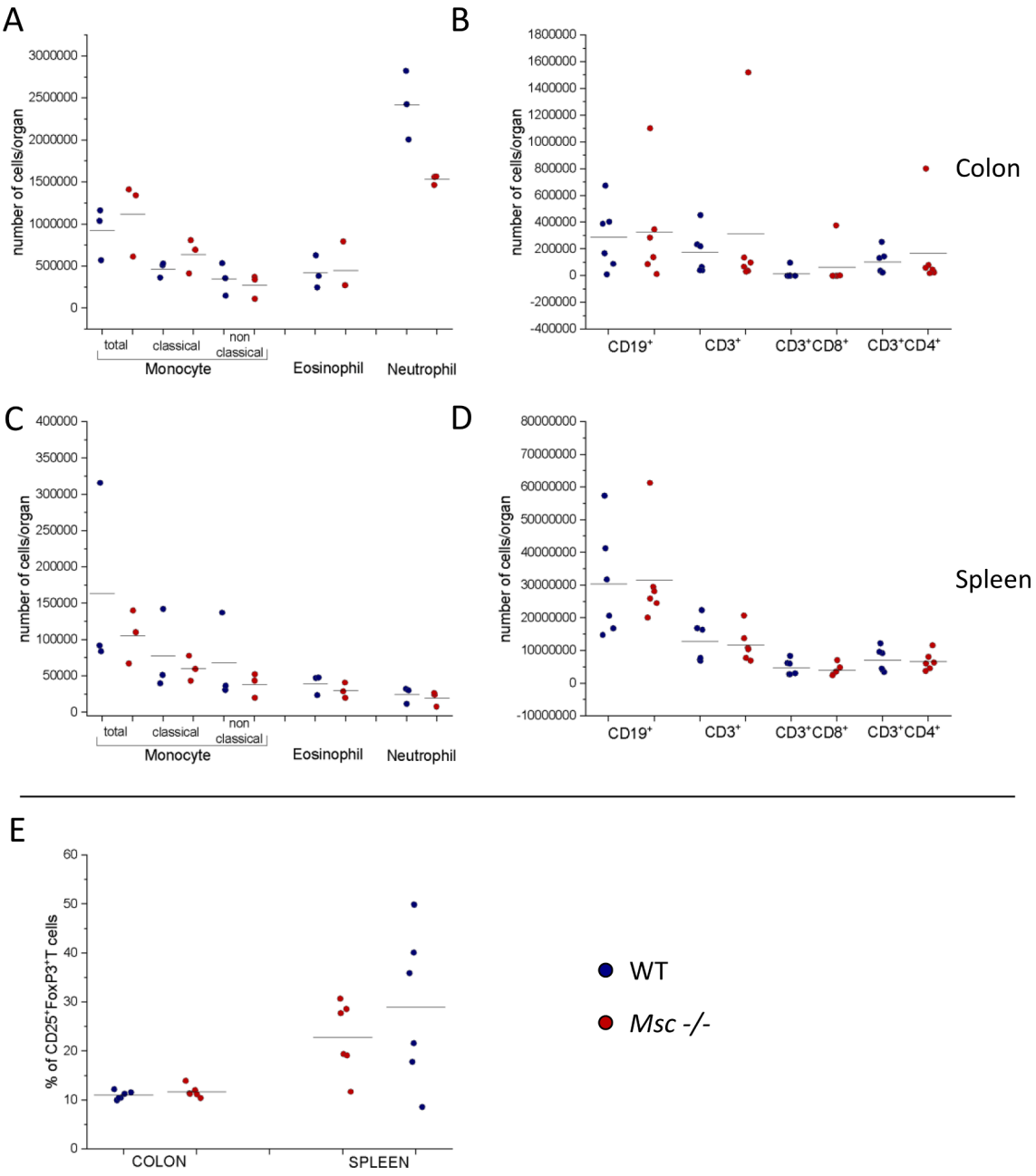

Fig. 5. *Msc gene knock-out does not impact the absolute cell number in spleen and colon of Msc $^{-/-}$ compared to WT DSS-colitis mice.* Panel shows the absolute cell number belonging to myeloid lineage (A, top left, colon; C, mid left, spleen) in WT (n=3, blue dots) and *Msc*$^{-/-}$ (n=3, red dots) or to lymphoid lineage (B, top right, colon; D, mid right, spleen) in WT (n=6, blue dots) and *Msc*$^{-/-}$ (n=6, red dots) mice, evaluated by means of a volumetric count at MACSquant® analyzer. (E) Percentage of FoxP3^{+}CD25^{+} cells in colon (left), spleen (right) in WT (n=6, blue dots) and *Msc*$^{-/-}$ (n=6, red dots). Horizontal black lines represent the mean value; Mann–Whitney test was used.

injury and higher levels of IL-17 and IL-22 produced by colonic cells [28, 29]. Multiple reasons might have contributed to this outcome: first, we used a 3% DSS solution, whereas in comparative studies mice were treated with 4% DSS. More importantly, different techniques and different organs were used for the evaluation of cytokines' production: indeed, Yu et al. [28] evaluated cytokines amount by ELISA and qRT-PCR in the supernatant from whole colonic tissue or Peyer's patches/mesenteric lymph nodes, respectively, whereas we only looked at cytokines produced by splenic and lymph nodal T cells by means of intracellular staining at flow cytometer. Moreover, in a brief letter, Yan et al. [30] found a higher production of IL-17A and IL-22 in FACS-sorted memory T cells from Msc$^{-/-}$ mice, but, again, in a different setting from ours. Nonetheless, considering the similar disease progression between the two groups in our experiments, comparable levels of IL-22 in the colon mucosa should not be unexpected, as IL-22 is mainly a cytokine involved in mucosal protection and pathology [31] Moreover, it is well known the influence of initial microbiota composition in the DSS colitis model, with several studies describing a microbiota-dependent severity in DSS-colitis, even using the same murine strain in repeated conditions [32–34].

Despite we are fully aware of the limitation introduced by lack of using littermate mice, our analysis of the microbiota profile revealed negligible differences between the two groups in the initial microbiota composition, suggesting that the presence/absence of the *Musculin* gene is not relevant for shaping microbiota composition during DSS establishment and course, regardless mice genetics. Conversely, when we

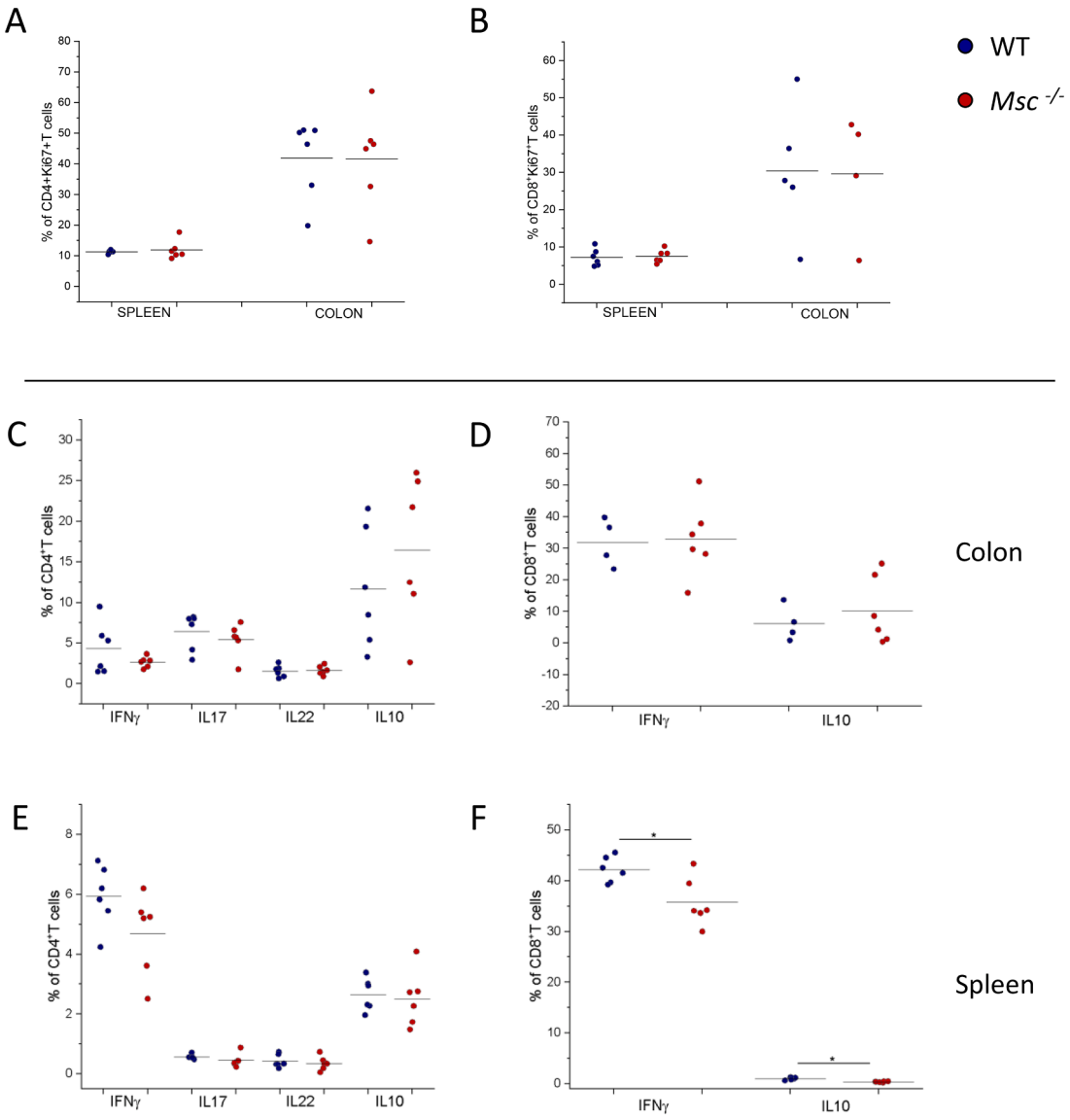

Fig. 6. *Msc gene knock-out does not affect the proliferative capability and has a minor impact on cytokines production in CD4+ and CD8+ in spleen and colon in Msc $^{-/-}$ compared to WT DSS-colitis mice.* (A) Proliferative capability of T cells expressed as percentage of $CD4^+Ki\text{-}67^+$ T cells from spleen WT (n=6, blue dots) and *Msc*$^{-/-}$ (n=6, red dots) and colon WT (n=6, blue dots) and *Msc*$^{-/-}$ (n=6, red dots) in DSS mice. (B) Proliferative capability of T cells expressed as percentage of $CD8^+Ki\text{-}67^+$ T cells from spleen WT (n=6, blue dots) and *Msc*$^{-/-}$ (n=6, red dots) and colon WT (n=5, blue dots) and *Msc*$^{-/-}$ (n=4, red dots) in DSS mice. (C, D) Percentage of total $CD4^+$ T or $CD8^+$ (E, F) T cells producing IL-2, IFN-γ, IL-17 or IL-22 after activation with PMA plus ionomycin and with brefeldin-A in colon (mid), spleen (bottom) in WT (n=6, blue dots) and *Msc*$^{-/-}$ (n=6, red dots) DSS mice, evaluated by means of intracytoplasmic staining at flow cytometer. Horizontal black lines represent the mean value; Mann–Whitney test was used (*$p < 0.05$).

compared the composition before and after the DSS treatment within the same experimental group, we appreciated a significant diversity, already at the phylum level, with some shared classes and families between WT and *Msc*$^{-/-}$ mice after DSS administration. Notably, we reported a marked dysbiotic status when comparing T0 vs T1 in both WT and *Msc*$^{-/-}$ mice, due at least to an increase of the mean *Proteobacteria* percentage, especially in the *Msc*$^{-/-}$ group. Interestingly, *Proteobacteria* is known to be a pro-inflammatory phylum and is often found to be increased in disease inflammatory conditions, such as IBD and DSS-induced colitis models [35–41], promoting the production of excessive pro-inflammatory cytokines [42,43]. Thus, our microbiota analysis reflected immunological data, with irrelevant differences between WT and *Msc*$^{-/-}$ mice after DSS disease, suggesting a scarce impact of *Msc* gene deletion in modulating colitis course and, on the other hand, the DSS ability to impact the gut microbiota composition within each group, without altering immune cells composition and, in particular, T cells' response.

However, despite the microbiota analysis showed a similar establishment of proinflammatory microbiota during DSS disease, the reduced submucosal cells infiltration might prelude to a faster recovery in *Msc*$^{-/-}$ mice, as we hypothesize for EAE model. Interestingly, the $CD8^+$ T cells produced less IFN-γ and IL-10 in the spleen, an organ not directly interested by the disease, as observed in the lymph nodes of EAE mice. Few studies have focused, so far, on the relevance of $CD8^+$ T cells in colitis model and, among them, Nancey et al. [44] described the expansion of cytotoxic IFN-γ producing $CD8^+$ cells in colon draining lymph nodes five days after BALB/c mice were challenged with a sub-optimal dose of 2,4-dinitrobenzene sulfonic acid, in a model of chemically-induced inflammatory colitis closely related to DSS [44].

However, we think that a later evaluation might be useful to highlight the potential *Msc* involvement in the clinical recovery from the diseases, in order to achieve a wider perspective on *Msc* role in

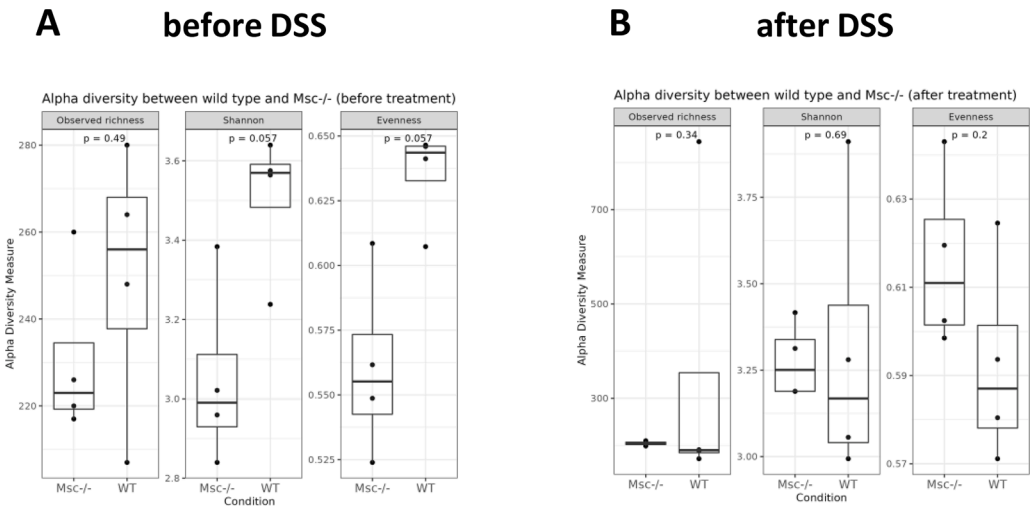

Fig. 7. *Genetic background does not alter the composition of mice microbiota.* Box plots show the alpha diversity (displayed by Observed richness, Shannon and Evenness indices), determined after 16S rRNA V3-V4 region gene sequencing on mice feces between *Msc*$^{-/-}$ and WT mice before (Fig.7A) and after (Fig.7B) the DSS treatment. Horizontal black line in the box represents the median; whiskers represent the interquartile range multiplied by 1.5; Wilcoxon rank-sum test was used (p-values < 0.05 were considered statistically significant).

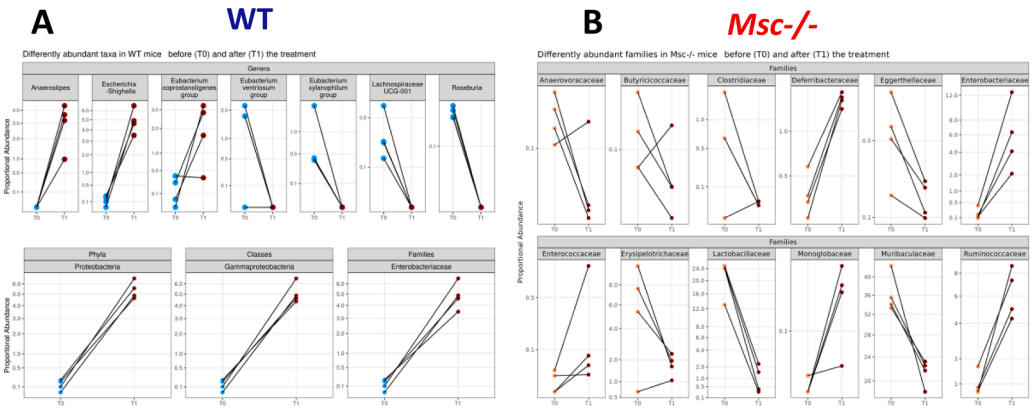

Fig. 8. *DSS-derived inflammation shape alike the gut microbiota in Msc*$^{-/-}$ *and WT mice, regardless genetic background.* Segment plots show the proportional abundance of main taxa after 16S rRNA V3-V4 region gene sequencing on mice feces, before and after the DSS treatment in WT (Fig.8A) and *Msc*$^{-/-}$ (Fig.8B). The abundances are displayed as square proportional abundances on the y-axis. Lines connect paired samples and highlight the differences in each abundance.

inflammatory context.

5. Conclusions

To our knowledge this is the first work addressing the role of *Msc* in EAE and our results indicated a very marginal role of *Msc* in EAE both in the onset and the early phase of diseases. More interestingly, the negligible role of *Msc* gene emerged also in DSS-colitis model, a toxic, chemically induced inflammatory model that does not need the priming with an antigen as the EAE. Here, the study also strengthened the immunological data with the assessment of the microbiota profile, demonstrating an irrelevant *Msc* role in shaping microbiota composition and, in turn, the immune regulation. In these models, the involvement of other pathological mechanisms implicated in T cell activation and expansion could explain the marginal role of the transcription factor *Msc* in disease onset. However, further studies to better elucidate the role of this transcription factor in autoimmunity and chronic inflammation are needed.

Declaration of Competing Interest

None.

Acknowledgments

The project has been granted by Multiple Sclerosis Italian Association (AISM) (project number 2017/R/3)

References

[1] S. Sozzani, M.P. Abbracchio, V. Annese, S. Danese, O. De Pità, G. De Sarro, S. Maione, I. Olivieri, A. Parodi, P. Sarzi-Puttini, Chronic inflammatory diseases: do immunological patterns drive the choice of biotechnology drugs? A critical review, Autoimmunity 47 (5) (2014) 287–306, https://doi.org/10.3109/08916934.2014.897333. AugEpub 2014 Apr 3. PMID: 24697663.

[2] C. Murre, Helix–loop–helix proteins and the advent of cellular diversity: 30 years of discovery, Genes Dev. 33 (2019) 6–25, https://doi.org/10.1101/gad.320663.118.

[3] M.E. Jones, Y. Zhuang, Acquisition of a functional T cell receptor during T lymphocyte development is enforced by HEB and E2A transcription factors, Immunity 27 (6) (2007) 860–870, https://doi.org/10.1016/j.immuni.2007.10.014. DecPMID: 18093538; PMCID: PMC2190753.

[4] I. Engel, C. Johns, G. Bain, R.R. Rivera, C. Murre, Early thymocyte development is regulated by modulation of E2A protein activity, J. Exp. Med. 194 (6) (2001) 733–745, https://doi.org/10.1084/jem.194.6.733. Sep 17PMID: 11560990; PMCID: PMC2195962.

[5] C. Murre, G. Bain, M.A. van Dijk, I. Engel, B.A. Furnari, M.E. Massari, J. R. Matthews, M.W. Quong, R.R. Rivera, M.H. Stuiver, Structure and function of helix-loop-helix proteins, Biochim. Biophys. Acta 1218 (2) (1994) 129–135, https://doi.org/10.1016/0167-4781(94)90001-9. Jun 21PMID: 8018712.

[6] C. Murre, The helix-loop-helix motif, Eds., in: F. Eckstein, D.M.J. Lilley (Eds.), The helix-loop-helix motif, Nucleic Acids and Molecular Biology 6 (1992), https://doi.org/10.1007/978-3-642-77356-3_6.

[7] Y.Y. Lin, M.E. Jones-Mason, M. Inoue, A. Lasorella, A. Iavarone, Q.J. Li, M. L. Shinohara, Y. Zhuang, Transcriptional regulator Id2 is required for the CD4 T cell immune response in the development of Experimental Autoimmune Encephalomyelitis, J. Immunol. 189 (3) (2012) 1400–1405, https://doi.org/10.4049/jimmunol.1200491. Aug 1Epub 2012 Jun 27. PMID: 22745378; PMCID: PMC3401239.

[8] C.Y. Yang, J.A. Best, J. Knell, E. Yang, A.D. Sheridan, A.K. Jesionek, H.S. Li, R. R. Rivera, K.C. Lind, L.M. D'Cruz, S.S. Watowich, C. Murre C, A.W. Goldrath, The transcriptional regulators Id2 and Id3 control the formation of distinct memory CD8+ T cell subsets, Nat. Immunol. 6 (12) (2011) 1221–1229, https://doi.org/10.1038/ni.2158. Nov12PMID: 22057289; PMCID: PMC3872000.

[9] J. Lu, R. Webb, J.A. Richardson, E.N. Olson, MyoR: a muscle restricted basic helix–loop–helix transcription factor that antagonizes the actions of MyoD, Proc. Natl. Acad. Sci. USA 96 (1999) 552–557.

[10] K. Hishikawa, T. Marumo, S. Miura, A. Nakanishi, Y. Matsuzaki, K. Shibata, T. Ichiyanagi, H. Kohike, T. Komori, I. Takahashi, O. Takase, N. Imai, M. Yoshikawa, T. Inowa, M. Hayashi, T. Nakaki, H. Nakauchi, H. Okano, T. Fujita, *Musculin*/MyoR is expressed in kidney side population cells and can regulate their function, J. Cell. Biol. 169 (6) (2005) 921–928, https://doi.org/10.1083/jcb.200412167.

[11] J.P. Harris, M. Bhakta, S. Bezprozvannaya, L. Wang, C. Lubczyk, E.N. Olson, N. V. Munshi, MyoR modulates cardiac conduction by repressing Gata4, Mol. Cell. Biol. 35 (4) (2015) 649–661, https://doi.org/10.1128/MCB.00860-14. FebEpub 2014 Dec 8. PMID: 25487574; PMCID: PMC4301724.

[12] F. Zhao, A. Vilardi, R.J. Neely, J.K. Choi, Promotion of cell cycle progression by basic helix-loop-helix E2A, Mol. Cell. Biol. 21 (2001) 6346–6357.

[13] R.A. Luchtel, M.T. Zimmermann, G. Hu, N. Oishi, H.K. Jacobs, Y. Zeng, T. Hundal, K.L. Rech, R.P. Ketterling, J.H. Lee, B.W. Eckloff, H. Yan, K.S. Gaonkar, S. Tian, Z. Ye, M.E. Kadin, J. Sidhu, L. Jiang, J. Voss, B.K. Link, S.I. Syrbu, F. Facchetti, N. N. Bennani, S.L. Slager, T. Ordog, J.P. Kocher, J.R. Cerhan, S.M. Ansell, A. L. Feldman, Recurrent MSCE116K mutations in ALK-negative anaplastic large cell lymphoma, Blood 133 (26) (2019) 2776–2789, https://doi.org/10.1182/blood.2019000626. Jun 27Epub 2019 May 17. PMID: 31101622; PMCID: PMC6598380.

[14] V. Santarlasci, A. Mazzoni, M. Capone, M.C. Rossi, L. Maggi, G. Montaini, B. Rossettini, R. Cimaz, M. Ramazzotti, G. Barra, R. De Palma, E. Maggi, F. Liotta, L. Cosmi, S. Romagnani, F. Annunziato, *Musculin* inhibits human T-helper 17 cell response to interleukin 2 by controlling STAT5B activity, Eur. J. Immunol. (2017), https://doi.org/10.1002/eji.201746996.

[15] C.A. Murphy, C.L. Langrish, Y. Chen, W. Blumenschein W, T. McClanahan, R. A. Kastelein, J.D. Sedgwick, D.J. Cua, Divergent pro- and antiinflammatory roles for IL-23 and IL-12 in joint autoimmune inflammation, J. Exp. Med. 198 (12) (2003) 1951–1957, https://doi.org/10.1084/jem.20030896. Dec 15Epub 2003 Dec 8. PMID: 14662908; PMCID: PMC2194162.

[16] C.L. Langrish, Y. Chen, W.M. Blumenschein, J. Mattson, B. Basham, D. Sedgwick, T. McClanahan, R.A. Kastelein, D.J. Cua, IL-23 drives a pathogenic T cell population that induces autoimmune inflammation, J. Exp. Med. 201 (2) (2005) 233–240, https://doi.org/10.1084/jem.20041257. Jan 17PMID: 15657292; PMCID: PMC2212798.

[17] Y. Chen, C.L. Langrish, B. McKenzie, B. Joyce-Shaikh, J.S. Stumhofer, T. McClanahan, W. Blumenschein, T. Churakovsa, J. Low, L. Presta, C.A. Hunter, R. A. Kastelein, D.J. Cua, Anti-IL-23 therapy inhibits multiple inflammatory pathways and ameliorates autoimmune encephalomyelitis, J. Clin. Invest. 116 (5) (2006) 1317–1326, https://doi.org/10.1172/JCI25308. MayPMID: 16670771; PMCID: PMC1450386.

[18] L. Cosmi, L. Maggi, V. Santarlasci, M. Capone, E. Cardilicchia, F. Frosali, V. Querci, R. Angeli, A. Matucci, M. Fambrini, F. Liotta, P. Parronchi, E. Maggi, S. Romagnani, F. Annunziato, Identification of a novel subset of human circulating memory CD4(+) T cells that produce both IL-17A and IL-4″, J. Allergy Clin. Immunol. 125 (2010) 222–230.

[19] L. Cosmi, R. De Palma, V. Santarlasci, L. Maggi, M. Capone, F. Frosali, G. Rodolico, V. Querci, G. Abbate, R. Angeli, L. Berrino, M. Fambrini, M. Caproni, F. Tonelli, E. Lazzeri, P. Parronchi, F. Liotta, E. Maggi, S. Romagnani, F. Annunziato, Human interleukin 17–producing cells originate from a CD161+CD4+ T cell precursor, J. Exp. Med. 205 (8) (2008) 1903–1916, https://doi.org/10.1084/jem.20080397.

[20] L. Cosmi, R. Cimaz, L. Maggi, V. Santarlasci, M. Capone, F. Borriello, F. Frosali, V. Querci, G. Simonini, G. Barra, M.P. Piccinni, F. Liotta, R. De Palma, E. Maggi, S. Romagnani, F. Annunziato, Evidence of the transient nature of the Th17 phenotype of CD4+CD161+ T cells in the synovial fluid of patients with juvenile idiopathic arthritis, Arthritis Rheum. 63 (2011) 2504–2515.

[21] C.W.Z. Chen, V. Dardalhon, S. Xiao, T. Thalhamer, M. Liao, A. Madi, R.F. Franca, T. Han, M. Oukka, V. Kuchroo, The transcription factor *Musculin* promotes the unidirectional development of peripheral Treg cells by suppressing the TH2 transcriptional program, Nat. Immunol. 18 (3) (2017) 344–353, volume 18.

[22] E. Russo, A. Taddei, M.N. Ringressi, F. Ricci, A. Amedei, The interplay between the microbiome and the adaptive immune response in cancer development, Therap. Adv. Gastroenterol. 9 (4) (2016) 594–605, https://doi.org/10.1177/1756283×16635082. Jul.

[23] E. Russo, G. Bacci, C. Chiellini, C. Fagorzi, E. Niccolai, A. Taddei, F. Ricci, M. N. Ringressi, R. Borrelli, F. Melli, M. Miloeva, P. Bechi, A. Mengoni, R. Fani, A. Amedei, Preliminary comparison of oral and intestinal human microbiota in patients with colorectal cancer: a pilot study, Front. Microbiol. 8 (2017) 2699.

[24] E. Russo, L. Cinci, L. Di Gloria, S. Baldi, M. D'Ambrosio, G. Nannini, E. Bigagli, L. Curini, M. Pallecchi, A.D. Arcese, S. Scaringi, C. Malentacchi, G. Bartolucci, M. Ramazzotti, C. Luceri, A. Amedei, F. Giudici, Crohn's disease recurrence updates: first surgery vs. surgical relapse patients display different profiles of ileal microbiota and systemic microbial-associated inflammatory factors, Front. Immunol. 13 (2022), 886468, https://doi.org/10.3389/fimmu.2022.886468. Jul 29.

[25] C.A. Dendrou, L. Fugger, M.A. Friese, Immunopathology of multiple sclerosis, Nat. Rev. Immunol. 15 (9) (2015) 545–558.

[26] W.J. Karpus, R.H. Swanborg, CD4+ suppressor cells differentially affect the production of IFN-gamma by effector cells of Experimental Autoimmune Encephalomyelitis, J. Immunol. 143 (11) (1989) 3492–3497.

[27] M. Koutrolos, K. Berer, N. Kawakami, H. Wekerle, G. Krishnamoorthy, Treg cells mediate recovery from EAE by controlling effector T cell proliferation and motility in the CNS, Acta Neuropathol. Commun. 2 (2014) 163, https://doi.org/10.1186/s40478-014-0163-1.

[28] J. Yu, Y. Liu, W. Zhang, X. Yang, W. Tang, H. Liang, S. Li, W. Gao, J. Yan, *Musculin* deficiency aggravates colonic injury and inflammation in mice with inflammatory bowel disease, Inflammation 43 (4) (2020) 1455–1463, https://doi.org/10.1007/s10753-020-01223-y. Aug.

[29] Y. Jun, Y. Jing, Y. Shunzong, T. Wanqi, M. We, Y. Xue, L. Yijia, L. Huaping, Z. Xuemei, S. Jing, C. Yang, M. Changchuin, N. Richard, G. Wenda, *Musculin* is highly enriched in Th17 and IL-22-producing ILC3s and restrains pro-inflammatory cytokines in murine colitis, Eur. J. Immunol. 51 (4) (2021) 995–998, https://doi.org/10.1002/eji.202048573. Apr.

[30] J. Yan, J. Yu, J. Yan, J. Yu, S. Yuan, W. Tang, W. Ma, X. Yang, Y. Liu, H. Liang, X. Zhong, J. Shao, Y. Cao, C. Mao, R. Near, W. Gao, *Musculin* is highly enriched in Th17 and IL-22-producing ILC3s and restrains pro-inflammatory cytokines in murine colitis, Eur. J. Immun. 51 (4) (2021) 995–998.

[31] H.X. Wei, B. Wang, B. Li, IL-10 and IL-22 in mucosal immunity: driving protection and pathology, Front. Immunol. 11 (2020) 1315, https://doi.org/10.3389/fimmu.2020.01315.

[32] M. Li, Y. Wu, Y. Hu, L. Zhao, C. Zhang, Initial gut microbiota structure affects sensitivity to DSS-induced colitis in a mouse model, Sci. China Life Sci. 61 (2018) 762–769.

[33] N.A. Nagalingam, J.Y. Kao, V.B. Young, Microbial ecology of the murine gut associated with the development of dextran sodium sulfate-induced colitis, Inflamm. Bowel Dis. 17 (4) (2011) 917–926, https://doi.org/10.1002/ibd.21462.

[34] M.M. Heimesaat, A. Fischer, B. Siegmund, A. Kupz, J. Niebergall, D. Fuchs, H. K. Jahn, M. Freudenberg, C. Loddenkemper, A. Batra, H.A. Lehr, O. Liesenfeld, M. Blaut, U.B. Göbel, Ralf R. Schumann, Stefan Bereswill, Shift towards pro-inflammatory intestinal bacteria aggravates acute murine colitis *via* Toll-like receptors 2 and 4″, PLOS One 2 (7) (2007) https://doi.org/10.1371/journal.pone.0000662 vol.

[35] D. Berry, O. Kuzyk, I. Rauch, S. Heider, C. Schwab, E. Hainz, T. Decker, M. Müller, B. Strobl, C. Schleper, T. Urich, M. Wagner, L. Kenner, A. Loy, Intestinal microbiota signatures associated with inflammation history in mice experiencing recurring colitis", Front. Microbiol. 6 (2015) 1408.

[36] N.R. Shin, T.W. Whon, J.W. Bae, Proteobacteria: microbial signature of dysbiosis in gut microbiota, Trends Biotechnol. 33 (9) (2015) 496–503.

[37] D.N. Frank, A.L. Amand, R.A. Feldman, E.C. Boedeker, N. Harpaz, N.R. Pace, Molecular-phylogenetic characterization of microbial community imbalances in human inflammatory bowel diseases, Proc. Natl. Acad. Sci. USA 104 (34) (2007) 13780–13785.

[38] C. Manichanh, L. Rigottier-Gois, E. Bonnaud, K. Gloux, E. Pelletier, L. Frangeul, R. Nalin, C. Jarrin, P. Chardon, P. Marteau, J. Roca, J. Dore, Reduced diversity of faecal microbiota in Crohn's disease revealed by a metagenomic approach, Gut 55 (2) (2006) 205–211, https://doi.org/10.1136/gut.2005.073817. Feb.

[39] U. Gophna, K. Sommerfeld, S. Gophna, W.F. Doolittle, S.J. Veldhuyzen van Zanten, Differences between tissue-associated intestinal microfloras of patients with Crohn's disease and ulcerative colitis, J. Clin. Microbiol. 44 (11) (2006) 4136–4141.

[40] X. Bian, W. Wu, L. Yang, L. Lv, Q. Wang, Y. Li, J. Ye, D. Fang, J. Wu J, X. Jiang, D. Shi, L. Li, Administration of akkermansia muciniphila ameliorates dextran sulfate sodium-induced ulcerative colitis in mice, Front. Microbiol. 10 (2019) 2259, vol.

[41] M. Constante, G. Fragoso, A. Calvé, M. Samba-Mondonga, M.M. Santos, Dietary Heme induces gut dysbiosis, aggravates colitis, and potentiates the development of adenomas in mice, Front. Microbiol 8 (2017) 1809, vol.

[42] Y. Qu, L. Xinyi, X. Fengying, Z. Shimin, W. Xuemei, W. Yuzhen, X. Jiming, Kaempferol alleviates murine experimental colitis by restoring gut microbiota and inhibiting the LPS-TLR4-NF-kappaB Axis", Front. Immunol. 12 (2021), 679897 vol.

[43] S.S. Mohamed, N.F. Abdeltawab, W. Wadie, L.A. Ahmed, R.M. Ammar, S. Rabini, H. Abdel-Aziz, M.T. Khayyal, Effect of the standard herbal preparation, STW5, treatment on dysbiosis induced by dextran sodium sulfate in experimental colitis, BMC Complement. Med. Ther. 21 (1) (2021) 168.

[44] S. Nancey, S. Holvöet, I. Graber, V. Desreumaux, B. Flourié, D. Kaiserlian, CD8+ cytotoxic T cells induce relapsing colitis in normal mice, Gastroenterology 131 (2) (2006) 485–496, https://doi.org/10.1053/j.gastro.2006.05.018. Aug.